

Quantitative Determination of the Radius of Gyration of Poly(methyl methacrylate) in the Amorphous Solid State by Time-Resolved Fluorescence Depolarization Measurements of Excitation Transport

K. A. Peterson, M. B. Zimmt, S. Linse, R. P. Domingue, and M. D. Fayer*

Department of Chemistry, Stanford University, Stanford, California 94305.
Received June 16, 1986

ABSTRACT: Excitation transport among naphthyl chromophores in low concentration on isolated coils of poly(2-vinylnaphthalene-co-methyl methacrylate) in a poly(methyl methacrylate) host is monitored by time-resolved fluorescence depolarization spectroscopy. Comparison of the experimental results to a recently developed theory for excitation transport in finite volume systems employing Gaussian segmental distribution functions allows the quantitative evaluation of the copolymer root-mean-square radius of gyration ($\langle R_g^2 \rangle^{1/2}$). The dependence of $\langle R_g^2 \rangle^{1/2}$ on the fraction of 2-vinylnaphthalene (2-VN) monomer in the copolymer is determined for three 23 000 M_w copolymers containing 9%, 6%, and 4% 2-VN. The measured $\langle R_g^2 \rangle^{1/2}$ are independent of 2-VN concentration. The $\langle R_g^2 \rangle^{1/2}$ values for the 23 000 M_w copolymers and a 60 000 M_w 9% 2-VN copolymer are identical with literature $\langle R_g^2 \rangle^{1/2}$ determinations for the same molecular weight PMMA polymers in Θ -solvents. The results demonstrate the quantitative utility of electronic excitation transport monitored by fluorescence depolarization spectroscopy as a tool for the determination of polymer conformation in the solid state.

I. Introduction

The macroscopic properties of solid-state polymer systems arise from the microscopic interaction of the individual polymer chains. The bulk properties of polymer blends are critically dependent on the mixing of blend components on a molecular level. Through the careful adjustment of the composition of blends technological advances in the engineering of polymer materials have been made.¹ In order to understand these systems more fully, it is desirable to investigate the interactions of individual polymer chains with the host environment.

A polymer coil in a solid blend can adopt a large number of configurations. The probability of any coil conformation depends on the thermodynamic interaction of the coil with its environment, on the geometric requirements of the allowed bond angles and rotations, and on the associated conformational entropy.² A change in the thermodynamic properties of the environment will lead to a change in the average chain conformation. A very sensitive indication of these thermodynamic interactions is the root-mean-square radius of gyration of a guest polymer dispersed in a polymer host matrix.

Currently, neutron scattering is the most common method used to determine $\langle R_g^2 \rangle^{1/2}$ of isolated polymer coils in the solid state. This technique has proven to be quite informative,³ and although it has the advantage of providing a direct probe of chain structure, its use suffers from a number of limitations. A monochromatic neutron source is required. In order to produce contrast, the polymer component being investigated, or the polymer host, must be deuteriated. The mechanical and thermodynamic properties of a number of polymers and polymer blends are strongly affected by deuteriation.⁴ It is difficult or impossible to assess the effect of deuteriation on neutron scattering measurements on polymer blends. Thus, conclusions drawn from the deuteriated systems do not rigorously apply to the hydrogenated blends. Finally, scattering from the host makes it difficult to investigate the behavior of the guest polymer at very low concentration (<1%). Many polymer blends undergo phase separation at even lower concentrations. For these systems in particular, neutron scattering is incapable of providing structural and thermodynamic properties of the isolated guest coil. The limitations of neutron scattering have

created an interest in the use of excitation transport techniques to study the properties of solid-state polymer systems.

The dependence of excitation transport on local chromophore concentration has been used to provide qualitative information on the characteristics of polymers in blends. Excimer fluorescence resulting from excitation transport has been employed to characterize polymer miscibility, phase separation, and the kinetics of spinodal decomposition.⁵ Qualitative characterization of phase separation in blends has also been investigated through transport with trapping experiments.⁶ In these experiments one polymer in the blend contains donor chromophores and the second contains acceptors. Selective excitation of the former and detection of the latter provide a qualitative measure of interpenetration of the two components.

Electronic excitation transport is very sensitive to the separation and orientation of chromophores. Techniques that monitor the rate of excitation transport among chromophores on a polymer chain are direct probes of the conformation. Recent experiments measuring fluorescence depolarization arising from excitation transport among chromophores on isolated guest coils in solid-state polymer blends demonstrated the feasibility of determining the relative size of individual chains in various host environments.⁷ As a consequence of the excellent signal-to-noise ratio achievable in optical experiments, excitation transport can be employed to investigate a minor component in a blend at concentrations several orders of magnitude smaller than is possible with neutron scattering techniques. This allows the study of isolated coils in both miscible blends and immiscible blends, which tend to phase separate at very low concentrations.

It is easy to understand, qualitatively, the relationship between the dynamics of excitation transport among chromophores randomly tagged in low concentration on an isolated polymer coil and the size of the coil.^{7a} An ensemble of tagged coils in a polymer blend will have some ensemble-averaged root-mean-square radius of gyration, $\langle R_g^2 \rangle^{1/2}$. If the thermodynamic interaction between the guest coils and the host is very favorable, $\langle R_g^2 \rangle^{1/2}$ will be large and the average distance between chromophores will be large. Since the rate of excitation transport depends

on $1/r^6$, where r is the chromophore separation, transport will be slow. If the same guest polymer is placed in a different host, in which the guest–host thermodynamic interactions are less favorable, the coils will contract in order to minimize guest–host interactions.² The average chromophore separation will decrease. This decrease leads to more rapid excitation transport. The $1/r^6$ rate dependence makes excitation transport observables very sensitive to small changes in $\langle R_g^2 \rangle^{1/2}$. A more detailed description of the relationship between $\langle R_g^2 \rangle^{1/2}$ and the experimental observables is given in section II.

In a manner somewhat analogous to the effect of deuteration on a neutron scattering experiment, it is likely that attachment of the chromophore labels necessary for excitation transport experiments will cause perturbations to the polymer chain conformation. However, as experimentally demonstrated in detail below, it is possible to assess the extent, if any, of such perturbations and change the amount of label present to either eliminate the effects or permit an extrapolation to zero chromophore concentration. This is not possible for the deuteration that is necessary in neutron scattering experiments.

In section IV we present the results of time-resolved fluorescence depolarization experiments that monitor the rate of donor-to-donor excitation transport on copolymers of methyl methacrylate and 2-vinylnaphthalene dispersed in a host matrix of poly(methyl methacrylate) (PMMA). The composition of the blends was such that the copolymer coils were isolated in the host. We studied copolymers at two different molecular weights. The experimental results were analyzed with a recently developed theory, which relates the rate of excitation transport to the coil size, and provide quantitative measurement of $\langle R_g^2 \rangle^{1/2}$ for the guest copolymers.⁸ The mole percent of naphthalene groups on the copolymers is low, and the effect on the chain conformation is small. The $\langle R_g^2 \rangle^{1/2}$ determined here agree well with values obtained for PMMA by light scattering in Θ -solvents. However, to ensure that there is no significant effect due to the presence of the naphthalene groups, experiments were performed on a series of copolymers of the same molecular weight but varying in the number of naphthalenes per polymer chain. The results demonstrate that the copolymer size is independent of the number of naphthalenes per coil for relatively low naphthalene concentrations.

II. Relation of Experimental Observables and Theory

In systems involving donor–donor excited–state transport, the fundamental quantity of theoretical and experimental interest is $G^s(t)$, the ensemble-averaged probability that an originally excited chromophore is excited at time t .⁹ $G^s(t)$ contains contributions from excitations that never leave the originally excited chromophore and from excitations that return to the initially excited chromophores after one or more transfer events. $G^s(t)$ does not contain loss of excitation due to lifetime (fluorescence) events. In this section we discuss how $G^s(t)$ can be obtained experimentally from time-resolved fluorescence depolarization data. The method used to calculate the theoretical $G^s(t)$ and its relationship to $\langle R_g^2 \rangle^{1/2}$ are also briefly described.

If a sample of randomly oriented chromophores is excited by a short pulse of plane polarized light, the decay of the fluorescence intensities polarized parallel ($I_{\parallel}(t)$) and perpendicular ($I_{\perp}(t)$) to the exciting light can be written as

$$I_{\parallel}(t) = e^{-t/\tau}(1 + 2r(t)) \quad I_{\perp}(t) = e^{-t/\tau}(1 - r(t)) \quad (1)$$

τ is the fluorescence lifetime, and $r(t)$ is the fluorescence

anisotropy. $r(t)$ contains information about all sources of depolarization. If the transition dipoles of the chromophores in a solid polymer matrix are randomly oriented, the main source of depolarization in these experiments is excitation transport. The initially excited ensemble is polarized along the direction of the excitation \vec{E} field and gives rise to polarized fluorescence. Transport occurs into an ensemble of chromophores with randomly distributed dipole directions, and the fluorescence becomes unpolarized. The random distribution is assured by the low concentration of the chromophores. To a slight extent, on the time scale of interest, depolarization also occurs as a result of chromophore motion. In this case the fluorescence anisotropy is approximately

$$r(t) = C\Phi(t)G^s(t) \quad (2)$$

where $\Phi(t)$ is the rotational correlation function which contains the effects due to motion of the chromophores. C is a time-independent constant that describes the degree of polarization of the excitation and emission transitions involved. There are two approximations in eq 2. The first is that the rotational and energy transport contributions to depolarization are independent. This is an excellent approximation for the very slow and small extent of rotational depolarization in polymer blends on the time scale of interest. The second approximation is that $G^s(t)$ decays to zero, resulting in complete depolarization; i.e., the irreversible transfer of excitation from the initially excited donor into the ensemble of unexcited donors results in total loss of polarization. For coils with a low concentration of randomly placed chromophores this is approximately true. The residual polarization is only 4%, which results in an insignificant error.¹⁰

In order to obtain $G^s(t)$ for a given polymer, experiments on two different samples must be performed. These samples differ only in that the guest copolymers have a different fraction of chromophore-containing monomers. Copolymer A is the polymer of interest and has an appreciable number of chromophores, such that excitation transport will occur. Its fluorescence anisotropy, $r_A(t)$, is given by eq 2. Copolymer B has such a small number of chromophores that excitation transport is negligible ($G^s(t) = 1$) and only chromophore motion contributes to the anisotropy

$$r_B(t) = C\Phi(t) \quad (3)$$

$G^s(t)$ arising from the excitation transport on copolymer A can be calculated from the two experimental anisotropies:

$$G^s(t) = r_A(t)/r_B(t) \quad (4)$$

This method of determining $G^s(t)$ has the advantage that detailed knowledge of the parameters C and $\Phi(t)$ is unnecessary. $r(t)$ for either copolymer can be obtained from the individual parallel and perpendicular components of the fluorescence intensity. From eq 1

$$r(t) = \frac{I_{\parallel}(t) - I_{\perp}(t)}{I_{\parallel}(t) + 2I_{\perp}(t)} \quad (5)$$

To obtain a value for $\langle R_g^2 \rangle^{1/2}$ of copolymer A, we compare the experimentally determined $G^s(t)$ to a theoretical calculation of $G^s(t)$ for the same copolymer. Once the molecular weight and number of chromophores are known (these can be independently determined), the theory has only one adjustable parameter. This parameter is directly related to $\langle R_g^2 \rangle^{1/2}$.

The theory employed to analyze the data presented here has been described in detail elsewhere.⁸ Only a brief

summary and the pertinent equations will be given here. Random-flight statistics with an appropriate statistical segment length¹¹ are employed to describe the average chain conformation of the copolymer chains. This model has been applied successfully to polymer coils in solution. For a polymer with chromophores randomly distributed along the chain, the chromophore distribution function can be modeled by

$$P_i(r_{12}) d\bar{r}_{12} = 4\pi r_{12}^2 \left\{ np'(r_{12}) + \frac{N-n-1}{N-1} \sum_{\substack{j=1 \\ j \neq i}}^N \left(\frac{3}{2\pi a^2 |i-j|} \right)^{3/2} \exp\left(\frac{-3r_{12}^2}{2a^2 |i-j|} \right) \right\} dr_{12} \quad (6)$$

Equation 6 describes the probability that a chromophore (labeled 2) on any chain segment j is a distance r_{12} from a chromophore (labeled 1) on chain segment i . \bar{N} and a are the number of statistical segments and the statistical segment length of the polymer, respectively. N is the total number of chromophores on the chain, and n is the average number of unexcited chromophores also on segment i . The second term on the right-hand side of eq 6 gives the contribution to the chromophore density at r_{12} from all chromophores not on segment i . The first term models the chromophore distribution ($p'(r_{12})$) around chromophore 1 due to other chromophores also on segment i . This is a very small contribution to the overall distribution function, and its form is not critical.⁸ Therefore, we chose a simple approximation for this distribution, assuming chromophore 1 was in the center of the segment and the other n chromophores are distributed randomly about this point.

$$\begin{aligned} p'(r_{12}) &= 1 & 0 < r_{12} < a/2 \\ p'(r_{12}) &= 0 & r_{12} > a/2 \end{aligned} \quad (7)$$

Excited-state transport has been described by many formalisms.^{9,12,13} The theory we employ to describe the rate of excitation transport among the chromophores on a finite length polymer chain is an adaptation of a first-order cumulant expansion method developed by Huber for isotropic solutions.¹³ Previously a number of theoretical methods have been applied to infinite length polymer chains.¹⁴ These treatments have used both density expansions and a first-order cumulant expansion. The first calculation of excitation transport in a finite size system employed a density expansion to examine the problem of chromophores randomly distributed in a spherical volume.¹⁵ The unique feature of a finite size system is that the dynamics of excitation transport depend on the point of initial excitation. In the spherical problem, an initial excitation at the center of the sphere will have a different $G^s(t)$ from that of an initial excitation near the surface of the sphere because of the distinct spatial distributions of unexcited chromophores surrounding each of these points.

In the treatment of the finite sphere problem, a density expansion was used to obtain an accurate approximation for $G_i^s(t)$, the loss of excitation probability from an initially excited chromophore located at position i . $G_i^s(t)$ was then averaged exactly over all possible initial positions i to yield an approximation for the experimental observable $G^s(t)$. While $G^s(t)$ is approximate, no additional approximations are involved in obtaining $G^s(t)$.

The first-order cumulant expansion has been applied to several problems besides chromophores randomly dis-

tributed in an infinite three-dimensional system. The problem of chromophores randomly distributed on a finite stack of planes has been treated recently.¹⁶ In this problem the excitation transport dynamics depend on which plane contains the initially excited chromophore. The first-order cumulant expansion was used to obtain an approximate expression for $G_i^s(t)$, where i is the label of the plane containing the initial excitation. The observable $G^s(t)$ is then found by averaging over the initial excitation conditions. This involves a sum over i . As in the sphere problem described above, $G_i^s(t)$ is approximate, but for the physical model considered, the average over i is performed exactly. The cumulant expansion was also used to reexamine the finite sphere problem.^{14c} The investigators chose to approximate $G^s(t)$ rather than $G_i^s(t)$ by the cumulant expansion. Unlike the original treatment of the sphere problem, this approach approximates the average over the position of the initial excitation.

The problem of excitation transport among chromophores randomly tagged in low concentration on a finite length polymer coil is also a finite volume problem. Initial excitation of a chromophore near an end of the chain results in dynamics different from that of excitation of a chromophore near the middle of the chain because of the distinct distributions of chromophores about these two points. Peterson and Fayer have applied the first-order cumulant expansion to this problem. The details of the calculations and demonstrations of its accuracy are reported in ref 8. These investigators chose to apply the cumulant expansion to $G_i^s(t)$, and then, within the context of the freely jointed chain model, they perform the average over the position of initial excitation exactly. This results in a more accurate approximation than applying the cumulant expansion to $G^s(t)$ directly, since it avoids the approximate average over the initial location of excitation.

Using the chromophore distribution function, $P_i(r_{12})$, performing the cumulant expansion, and then averaging over the possible positions of the initially excited chromophore, we obtained an expression for $G^s(t)$ ⁸

$$G^s(t) = \frac{1}{N} \sum_{i=1}^N \exp \left[\frac{4\pi}{2} \int_0^\infty (1 - e^{-2\omega_{12}t}) P_i(r_{12}) r_{12}^2 dr_{12} \right] \quad (8)$$

ω_{12} is the rate of excitation transport between two chromophores at a separation of r_{12} . In eq 8, the exponential term is $G_i^s(t)$ and the sum over i (chain segments) is the average over the initial positions of excitation.

For rapidly rotating chromophores ω_{12} is given by¹⁷

$$\omega_{12} = \left(\frac{R_0}{r_{12}} \right)^6 / \tau \quad (9)$$

τ is the fluorescence lifetime and R_0 is the critical transfer radius. Equation 9 is the orientation-averaged expression for dipole-dipole interactions and is applicable to dynamic systems (e.g., chromophores in solution). For the experiments in this paper, the chromophores are essentially static, and R_0 in eq 9 must be replaced by

$$R_0' = (\gamma_2)^{1/3} R_0 \quad (10)$$

where $\gamma_2 = 0.8468$.^{14,18} Provided the molecular weight of the copolymer is known, eq 8 has only one adjustable parameter, the statistical segment length a . This is directly related to $\langle R_g^2 \rangle^{1/2}$ by

$$\langle R_g^2 \rangle = \frac{1}{6} (\bar{N} a^2) \quad (11)$$

Thus, a fit of the experimentally determined $G^s(t)$ with

Table I
Copolymer Characteristics

copolymer	mole fraction		M_w/M_n	av no. chromophores/chain
	2-VN	mol wt		
I	0.0015	~50 000	~2.5	<1
4-23	0.040	22 700	1.4	9 ± 1
6-22	0.059	22 400	1.5	13 ± 2
9-23	0.087	23 400	1.5	20 ± 1
9-60	0.087	59 800	1.3	49 ± 2

a theoretically calculated $G^*(t)$ determined by adjusting the statistical segment length will give a measure of $(R_g^2)^{1/2}$ for the copolymer.

III. Experimental Section

A. Polymer Materials. Five copolymers of methyl methacrylate (MMA) and 2-vinylnaphthalene (2-VN) were used in the fluorescence depolarization experiments. All were polymerized in benzene at 60 °C under nitrogen following the procedure of Fox et al.¹⁹ AIBN and butylthiol were used as initiator and chain-transfer reagent, respectively. The MMA (Aldrich) was washed with 5% NaOH, dried over NaSO₄, and vacuum distilled. The 2-VN (Aldrich) was recrystallized three times from ethanol and sublimed once. The AIBN was recrystallized from ethyl acetate. The copolymers were recovered from the reaction mixture by precipitation into methanol and subsequently washed several times with cold methanol.

The desired molecular weight fractions were obtained from the resulting polydisperse copolymers by size exclusion chromatography using Sephacryl S-200 resin and THF as eluent. The molecular weights of the fractions were determined on a Waters Associates analytic GPC using THF as eluent. The GPC instrument was calibrated by using nearly monodisperse PMMA standards (Pressure Chemical, $M_w/M_n < 1.1$). The copolymer used to determine the depolarization due to chromophore motion (0.0015 mol fraction 2-VN) was not fractionated. Its average molecular weight was determined by viscosity measurements. The mole fractions of vinylnaphthalene monomer units in the copolymers were determined by absorption spectroscopy at 320 nm (Cary 17 spectrometer), based on a molar extinction coefficient of 400 mol cm/L measured for ethylnaphthalene. Table I gives a summary of the characteristics for the five copolymers. The host polymer for all the blends was PMMA (Polysciences no. 4553, number-average molecular weight ~120 000).

B. Sample Preparation. All samples were solid blends of the desired guest copolymer and the host PMMA prepared by molding in a stainless steel piston above the glass transition temperature. The procedure is the same as described previously.^{7b} The samples were optically clear with no significant birefringence along the direction in which the pressure was applied. This was checked by viewing the samples through a polarizing microscope.

C. Data Acquisition. Figure 1 shows the experimental apparatus. The frequency-doubled (532 nm) output of an acousto-optically mode-locked, Q-switched Nd:YAG laser was used to synchronously pump a dye laser. The dye laser was cavity dumped with a Pockels cell to produce a single pulse at 640 nm, which was then frequency-doubled to give the ~25-ps excitation pulse at 320 nm. A small fraction of each UV excitation pulse was measured with a phototube and sample and hold circuit and recorded by computer so the fluorescence intensity could be normalized to the laser intensity. This eliminates effects due to laser intensity drift. The spot size of the excitation pulse at the sample was of the order of 1 mm, and the pulse energies were typically 0.5–1 μJ. The optical density of all samples was ≤0.2 at 320 nm. No significant reabsorption of fluorescence occurs in this OD range. The dependence of the recorded fluorescence intensity on the excitation intensity was linear, assuring that the microchannel plate was not saturated and the sample was not being bleached.

Fluorescence from the sample was focused into a monochromator with an interference filter and polarizer on the entrance slit. A microchannel plate (Hamamatsu R1645U-01) coupled to a transient digitizer (Tektronix Model R7912) detected the fluorescence at 337 nm. A computer was used to store the

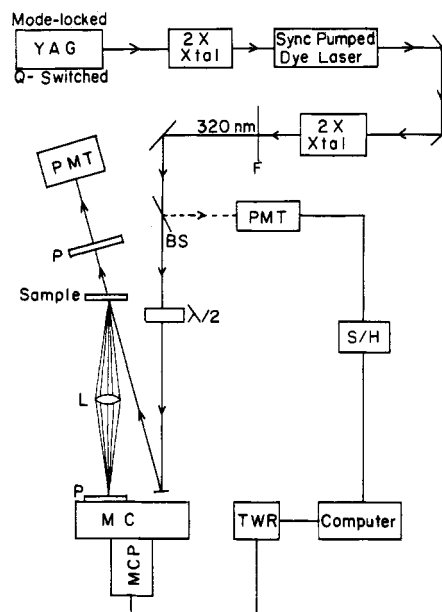


Figure 1. Experimental setup. The output of a mode-locked and Q-switched Nd:YAG laser is frequency-doubled and synchronously pumps a dye laser. The dye laser output is doubled to 320 nm for excitation. The polarization of the excitation beam is controlled by a half-wave plate. The fluorescence from the sample is collected by a lens, passed through a polarizer and a monochromator, and detected by a multichannel plate coupled to a transient waveform recorder. See text for further details. BS = beam splitter, PMT = photomultiplier tube, $\lambda/2$ = half-wave plate, S/H = sample and hold circuit, P = polarizer, L = lens, MC = monochromator, MCP = multichannel plate detector, TWR = transient waveform recorder, F = UV transmitting filter, and 2 × Xtal = second harmonic generating crystal.

fluorescence decays and average many decays to improve signal-to-noise ratios. The time resolution of the detection system was 1.0 ns.

$I_{\parallel}(t)$ and $I_{\perp}(t)$ were measured by rotating the polarization of the excitation pulse with a half-wave plate and keeping the detector polarizer unchanged at vertical polarization. Since the detection efficiency of the monochromator and microchannel plate can vary with the polarization of the light, this method ensures that the absolute ratio of $I_{\parallel}(t)$ to $I_{\perp}(t)$ is preserved. For a typical sample, 100 fluorescence decays at a given excitation polarization were collected and added by the computer. The excitation polarization was then rotated, and an additional 100 decays were collected, added, and stored separately by the computer. This sequence was repeated, and the additional data were added to the previously collected decays of the appropriate polarization until a total of 1000 decays at each polarization were collected. By use of eq 5, $r(t)$ is then calculated for this set of $I_{\parallel}(t)$ and $I_{\perp}(t)$ decays. The entire sequence was repeated for the same spot and different spots on the same sample. No substantial or systematic differences were observed. The $r(t)$ curves calculated from these separate data sets were then averaged together. Switching frequently between collecting fluorescence at the two polarizations minimizes any possible artifacts.

In addition to checking the birefringence of the samples in a polarizing microscope, the birefringence of the spot actually excited by the laser beam was checked by placing a polarizer and phototube in the excitation beam after the sample and measuring the ratio of the transmitted light parallel and perpendicular to the incident polarization. This ratio was 200:1 or higher for all samples and is large enough to ensure that there is no distortion in the data due to birefringence in the samples. Fluorescence data were also collected on samples of pure PMMA host material. The fluorescence from these samples was negligible compared to the fluorescence from the copolymer-containing samples.

D. Data Analysis. The experimental $r(t)$ and $G^*(t)$ were obtained from $I_{\parallel}(t)$ and $I_{\perp}(t)$ by the point-by-point calculations of eq 4 and 5. For an accurate comparison of the experimental curves with theoretical $G^*(t)$ curves calculated from eq 6–10, the

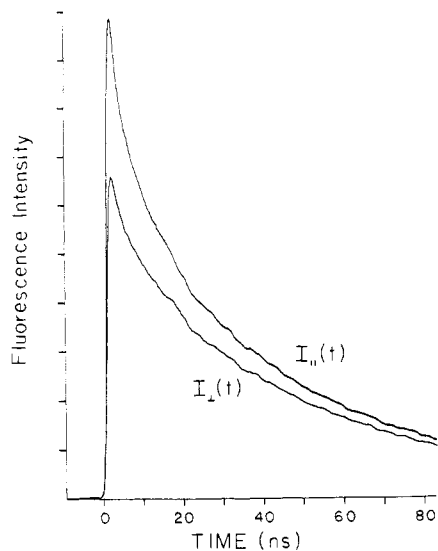


Figure 2. Polarized fluorescence decays for detection parallel ($I_{\parallel}(t)$) and perpendicular ($I_{\perp}(t)$) to the excitation polarization. The sample is copolymer 9-23 (23 400 M_w , 0.087 mol fraction 2-VN) in a 120 000 M_w PMMA host. Copolymer concentration is 0.38 wt %.

experimental apparatus impulse response must be appropriately convolved with the theoretical $G^s(t)$. This is done by convolving theoretical expressions for $I_{\parallel}(t)$ and $I_{\perp}(t)$ (calculated from the theoretical $G^s(t)$ curves by eq 1-3 with $\Phi(t) = 1$) with the apparatus response function. For this system the response function is well approximated as Gaussian with fwhm = 1 ns.^{7b} The theoretical $G^s(t)$ with the convolution is then calculated from these new $I_{\parallel}(t)$ and $I_{\perp}(t)$ curves with eq 4 and 5.

For the theory described in section II, $\langle R_g^2 \rangle^{1/2}$ is a linear function of R_0 . R_0 for the naphthalene chromophores on the copolymer chains dispersed in PMMA was determined previously^{7b} to be $13.0 \pm 0.6 \text{ \AA}$. This is the orientation-averaged R_0 which must be modified for the solid state as described in section II.

IV. Results and Discussion

Earlier experiments have shown the utility of excitation transport measurements in providing relative information regarding coil size in polymer blends.^{7b} The results of the experiments described here demonstrate that monitoring excitation transport on isolated coils in solid blends through time-resolved fluorescence depolarization techniques provides a quantitative measure of $\langle R_g^2 \rangle^{1/2}$ for the guest polymer. Experiments on different molecular weight guest copolymers are necessary to show the general applicability of the theory relating $G^s(t)$ to $\langle R_g^2 \rangle^{1/2}$ and to confirm the utility of assuming a Gaussian segment distribution for PMMA. Since the presence of the naphthalene groups could perturb the average chain conformation, $\langle R_g^2 \rangle^{1/2}$ was determined for a series of copolymers of essentially the same molecular weight but differing in the average number of naphthalenes on the chains.

A. Determination of $\langle R_g^2 \rangle^{1/2}$ for Copolymers of Different Molecular Weights. Time-resolved fluorescence depolarization experiments were performed on samples made from copolymer 9-23 (0.087 mol fraction 2-VN, 23 400 M_w) and from copolymer 9-60 (0.087 mol fraction 2-VN, 59 800 M_w) in 120 000 M_w PMMA. In both cases, the amount of copolymer in the host polymer was 3/8 wt %. It has been determined previously that for a 20 000 M_w copolymer of this type, this individual copolymer coils were isolated in PMMA at this concentration.^{7b} We determined that the copolymer 9-60 coils were also isolated at this concentration since a sample with 1/8 wt % of this copolymer gives the same anisotropy decay

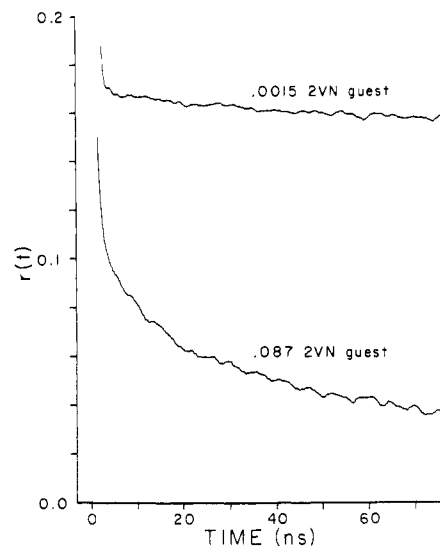


Figure 3. Fluorescence anisotropies, $r(t)$, calculated from experimental $I_{\parallel}(t)$ and $I_{\perp}(t)$ (see eq 5). The upper curve is a copolymer with a very small mole fraction (0.0015) of 2-vinylnaphthalene (copolymer I). Excitation transport does not occur, and the time dependence is due to very slow rotational depolarization (see eq 3). The lower curve is from the data shown in Figure 2. Here, the time-dependent depolarization is due to both excitation transport and the small amount of rotational depolarization (see eq 2).

as a sample with 3/8 wt % of the copolymer.

Figure 2 shows the polarized fluorescence decays ($I_{\parallel}(t)$ and $I_{\perp}(t)$) for the copolymer 9-23/PMMA blend. Figure 3 (lower curve) shows the fluorescence anisotropy, $r(t)$, calculated from the data by using eq 5. Also shown (upper curve) is $r(t)$ obtained in the same manner for the 0.0015 mol fraction 2-VN copolymer (copolymer I in Table I). The sample consists of 12% by weight of copolymer I. This sample contains so few chromophores that depolarization occurs solely as a result of chromophore motion. There is no excitation transport.

As discussed in section II, to obtain the experimental $G^s(t)$ for copolymer 9-23, it is necessary to take the ratio of the anisotropies of copolymer 9-23 to copolymer I. The resulting experimental $G^s(t)$ curve is shown in Figure 4. Figure 5 shows the experimental $G^s(t)$ obtained in the same manner for copolymer 9-60. In both these figures, we also show the best fits (smooth curves) obtained from the theory described in section II. Variation of the single adjustable parameter, the statistical segment length a , results in $\langle R_g^2 \rangle^{1/2}$ of 37 ± 3 and $61 \pm 3 \text{ \AA}$ for the 23 400 and 59 800 M_w copolymers, respectively. The sensitivity of the technique is demonstrated by theoretical curves at $\pm 2 \text{ \AA}$ from the best fits.

The measured $\langle R_g^2 \rangle^{1/2}$ for these two polymers varies with the square root of the chain length. This is as expected for flexible coils¹¹ and indicates that the Gaussian segment distribution function utilized in the analysis of the data is applicable to these copolymers. Neutron scattering experiments on isolated PMMA coils in a deuterated PMMA host show this same scaling of $\langle R_g^2 \rangle^{1/2}$ with molecular weight.^{3e}

Since these blends are essentially PMMA in PMMA, the copolymers are approximately in Θ -conditions.²⁰ (The effect of the naphthalene groups is discussed below.) True Θ -conditions for a solid blend would be PMMA in a PMMA host of the same molecular weight. We do not expect that a host M_w of 120 000 results in a significant deviation from Θ -conditions since, in a previous fluorescence depolarization experiment, nearly identical $r(t)$

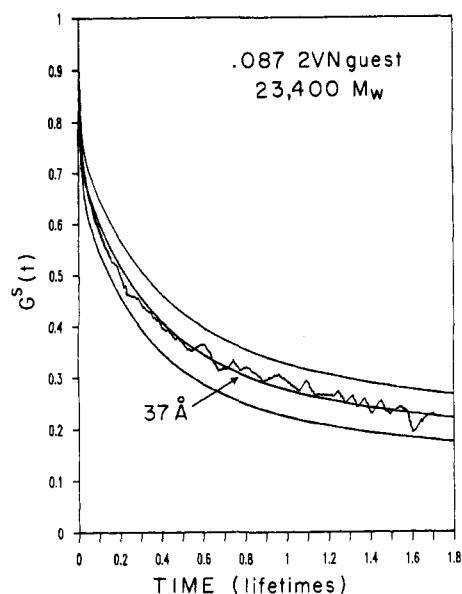


Figure 4. The quantity of experimental and theoretical interest is $G^s(t)$, the ensemble-averaged probability that the excitation is on the originally excited chromophore at time t . The experimental $G^s(t)$ results from taking the ratio of the lower to the upper anisotropy curves in Figure 3 (see eq 4). Also shown are theoretical $G^s(t)$ curves calculated by using eq 8 for a 23 400 M_w PMMA chain with 20 naphthalenes. The best fit, obtained by adjusting the statistical segment length a , results in an $\langle R_g^2 \rangle^{1/2}$ of 37 Å. This result is in close agreement with light scattering determinations of $\langle R_g^2 \rangle^{1/2}$ for a PMMA coil in a Θ -condition media. Also shown are theoretical curves at 39 (upper) and 35 Å (lower).

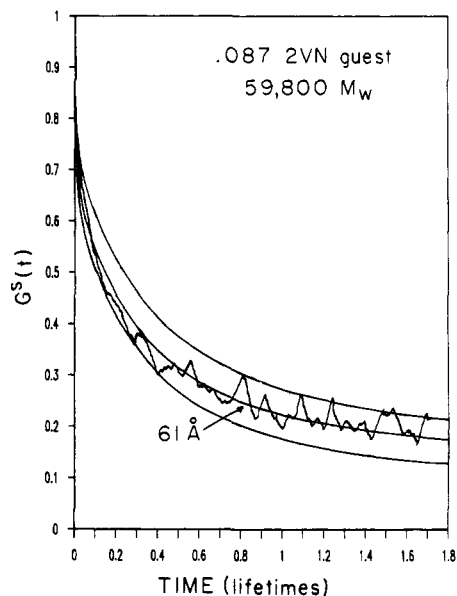


Figure 5. $G^s(t)$, the ensemble-averaged probability of finding the excitation on the originally excited chromophore. The experimental $G^s(t)$ is for copolymer 9-60 (59 800 M_w , 0.087 mol fraction 2-VN) in a 120 000 M_w PMMA host. The theoretical $G^s(t)$ curves are for a 59 800 M_w PMMA chain with 49 naphthalenes. The best fit yields an $\langle R_g^2 \rangle^{1/2}$ of 61 Å. The result is in very good agreement with other methods for determining $\langle R_g^2 \rangle^{1/2}$ of Θ -condition PMMA. The upper and lower theoretical curves are for 63 and 59 Å, respectively.

curves were obtained for a 20 000 M_w 2-VN/MMA copolymer in both 20 000 and 120 000 M_w PMMA hosts.^{7b} Assuming that these copolymers are essentially PMMA at Θ -conditions, it is possible to compare these results with light scattering measurements of $\langle R_g^2 \rangle^{1/2}$ for equivalent molecular weight PMMA in Θ -solvents. The values can be easily calculated from tabulated data.²¹ For 23 000 and

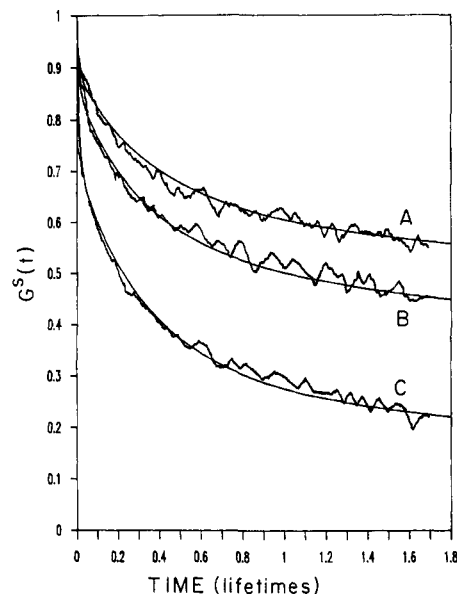


Figure 6. $G^s(t)$, the ensemble-averaged probability that the excitation is still on the originally excited chromophore. Data is shown for three copolymers of essentially the same molecular weight but differing in mole fraction of 2-VN. Curve A is copolymer 4-23 (22 700 M_w , 0.04 mol fraction 2-VN), curve B is copolymer 6-22 (22 400 M_w , 0.059 mol fraction 2-VN), and curve C is copolymer 9-23 (23 400 M_w , 0.087 mol fraction 2-VN). Also shown are the best-fit theoretical $G^s(t)$ curves for equivalent molecular weight PMMA chains with the appropriate number of naphthalenes. The resulting values for $\langle R_g^2 \rangle^{1/2}$ are 38, 39, and 37 Å in order from A to C. These results show that the presence of the naphthalene-containing monomers does not significantly perturb the average chain dimensions at least up to concentrations of 9 mol % 2-VN.

60 000 M_w PMMA at Θ -condition, $\langle R_g^2 \rangle^{1/2}$ should be 39 ± 4 and 64 ± 7 Å, respectively. The results from the excitation transport experiments are in excellent agreement with these values.

B. Effect of the Presence of Naphthalene Groups. Although the results for the two copolymers with 0.087 mol fraction naphthalene-containing monomers agree very well with other determinations of $\langle R_g^2 \rangle^{1/2}$ for Θ -condition PMMA, it is still necessary to ascertain that the presence of the chromophores does not significantly perturb the average chain conformation. This was accomplished by obtaining experimental $G^s(t)$ curves for three copolymers of essentially the same molecular weight, but varying in the amount of naphthalene in the chains. These three copolymers are designated 9-23, 6-22, and 4-23 in Table I and contain 8.7, 5.9, and 4.0 mol % naphthalene-containing monomers, respectively. The samples consisted of 3/8 weight % of the desired copolymer in the 120 000 M_w host PMMA. Figure 6 shows the experimental $G^s(t)$ curves obtained for these copolymers along with the theoretical best fits. The resulting values for $\langle R_g^2 \rangle^{1/2}$ are 37 ± 3 , 39 ± 3 , and 38 ± 3 Å for the three copolymers in order from the highest to the lowest naphthalene content. These results are in quantitative agreement with solution $\langle R_g^2 \rangle^{1/2}$ measurements under Θ -conditions. In addition, these results indicate that the presence of the naphthalene-containing monomers does not significantly perturb the average coil dimensions, at least up to naphthalene concentrations of 9 mol %.

Table II summarizes the results for the various copolymers in this study. A comment on the error bars associated with the measurements of $\langle R_g^2 \rangle^{1/2}$ in this study is necessary. The theoretical $G^s(t)$ curves at ± 2 Å shown in Figures 4 and 5 are to show the sensitivity of $G^s(t)$ to

Table II
Summary of Results

copolymer	$\langle R_g^2 \rangle^{1/2}$ determined by excitation transport	$\langle R_g^2 \rangle^{1/2}$ for equivalent M_w Θ -condition PMMA ^a
4-23	38 ± 3	39 ± 4
6-22	39 ± 3	39 ± 4
9-23	37 ± 3	39 ± 4
9-60	61 ± 3	64 ± 7

^a From reported literature values from light scattering measurements on PMMA in various Θ -solvents.²¹

small changes in $\langle R_g^2 \rangle^{1/2}$. The reported errors in Table II are estimated from errors in the measurement of the average number of naphthalenes per chain and the weight-average molecular weight. The fact that there is really a distribution of the number of chromophores and the molecular weight does not significantly effect the result.⁸ The molecular weight distribution can be controlled and tested during sample preparation. The samples used in this study have sufficiently narrow molecular weight distributions to avoid problems. The effect of the distribution in the number of chromophores per chain about the average number has been tested by theoretical calculations and shown to be insignificant.⁸ However, error in the determination of their average values, especially in the number of chromophores per chain for the smaller copolymers can lead to errors of a few angstroms in the theoretical fit.

V. Comments and Conclusion

The accuracy of the analysis presented in this paper is determined by the validity of two key approximations: (1) the description of the energy-transfer dynamics by the first-order cumulant expansion method and (2) the use of a Gaussian chromophore pair distribution function. Although originally developed for¹³ and successfully applied to the problem of energy transfer in disordered infinite volume systems, the cumulant method can be modified to provide a highly accurate description of energy transfer in finite volume systems such as polymer coils. The modification of the method to describe transfer in finite volume polymer systems has been described previously.⁸ For the number of chromophores and time scale involved in these experiments, the method is essentially exact.

Gaussian pair distribution functions are commonly employed in calculations involving freely jointed chains. Except in the limit of infinitely long polymer molecules, this description is approximate. For large chains, the use of a Gaussian distribution function is considered a very reasonable model, but for the moderate size chains studied here, the question remains open. The calculated $G^s(t)$ curves are very sensitive to $\langle R_g^2 \rangle^{1/2}$ and, as such, provide a test of the distribution functions employed. The quantitative agreement between the Θ -condition $\langle R_g^2 \rangle^{1/2}$ values determined for the 23 000 and 60 000 M_w polymer coils in solid and solution states shows that the Gaussian pair distribution function is adequate to describe these chains.

The theoretical analysis used in this paper to derive $\langle R_g^2 \rangle^{1/2}$ from the data is sufficiently powerful and flexible that transport observables for any pair distribution function can be calculated simply by replacing the Gaussian pair distribution function in eq 6. In fact, use of the theory in conjunction with a series of depolarization experiments covering a wide range of polymer types and molecular weights could serve to determine the applicability of the segmental distributions functions proposed for various types of polymers. However, it is necessary to

be careful in drawing conclusions about model pair-correlation functions based on the qualitative shape of the theoretical $G^s(t)$ curves alone. The experiment examines the pair-correlation function over a distance scale of several R_0 . The shape of the $G^s(t)$ curves may not change significantly with the use of different mathematical models. Previous theories by Fredrickson, Andersen, and Frank¹⁴ and by Ediger and Fayer^{7a} also predict the shape of $G^s(t)$ correctly for the types of polymer blends studied here, but are in error in the quantitative determination of $\langle R_g^2 \rangle^{1/2}$. The finite nature of the polymer chains, which restricts the volume in which the chromophores can reside and consequently results in an inequivalence among possible chromophore positions, strongly influences the general shape of the $G^s(t)$ curves. $G^s(t)$ curves calculated for freely jointed chains in this paper differ significantly from both theoretical and experimental $G^s(t)$ curves obtained for random isotropic chromophore distributions.^{7b} However, it is expected that $G^s(t)$ curves obtained, for example, for rigid rods will have a general shape quite different from those for freely jointed chains. When possible, it is useful to check the validity of the chromophore distribution model employed by making quantitative comparisons of excitation-transfer results to structural determinations by other methods such as light scattering.

These experiments demonstrate the utility of this excitation transport technique in the study of polymer blends. The technique allows quantitative determination of $\langle R_g^2 \rangle^{1/2}$ for isolated guest coils in a polymer matrix. The accuracy of the measurements is comparable to determinations performed with neutron scattering methods. However, we believe that the excitation-transfer technique offers greater flexibility in two ways. First, the signal-to-noise ratio achievable in excitation-transport experiments allows measurements on blends with guest polymer concentrations that are 1 or more orders of magnitude lower than the sensitivity limits of neutron scattering. Second, and most importantly, the effect of the labeled monomer on the copolymer conformation can be ascertained by performing a series of experiments on copolymers containing various mole fractions of label. Despite the insensitivity of the present results to the mole fraction of 2-VN, label concentration dependence studies must be performed on every blend system in order to quantify the effect of label-induced perturbation. This control is not readily available to neutron scattering experiments on solid-state polymer systems.

In these experiments, we have determined $\langle R_g^2 \rangle^{1/2}$ for PMMA in the solid state under Θ -conditions. The techniques and theory employed are easily extended to other solid-state systems, for example, miscible blends, phase-separated blends, or solvent-cast systems retaining substantial solvent. The effect of sample processing and history on coil conformation can also be probed. The sensitivity of excitation-transport observables to small changes in chromophore distribution coupled with the relative simplicity of time-resolved fluorescence experiments and the flexibility of the transport theory makes excitation transport induced fluorescence depolarization spectroscopy a valuable and unique tool for the study of solid-state polymer systems.

Acknowledgment. This work was supported by the Department of Energy, Office of Basic Energy Sciences (DE-FG03-84ER13251). Additional equipment support was provided by the National Science Foundation, Division of Materials Research (DMR84-16343), and the Stanford National Science Foundation Center for Materials Research. K.A.P. thanks the I.B.M. Corp. for a Predoctoral

Fellowship. Invaluable discussions with Professors C. W. Frank and M. D. Ediger and with Dr. J. Baumann as well as the members of the Stanford Center for Materials Research Polymer Thrust Program are gratefully acknowledged.

Registry No. (2-VN)(MMA) (copolymer), 53640-71-4; PMMA, 9011-14-7.

References and Notes

- (1) A number of good treatises exist: (a) Paul, D. R., Sperling, L. H., Eds. *Multicomponent Polymer Materials*; Advances in Chemistry Series 211; American Chemical Society: Washington, DC, 1986. (b) Solc, K., Ed. *Polymer Compatibility and Incompatibility: Principles and Practices*; MMI Press Symposium; Harwood Academic: New York, 1982; Vol. 2. (c) Olabisi, O.; Robeson, L. M.; Shaw, M. T. *Polymer-Polymer Miscibility*; Academic: New York, 1979. (d) Paul, D. R., Newman, S., Eds. *Polymer Chemistry*; Academic: New York, 1978; Vol. 1 and 2.
- (2) Flory, P. J. *Principles of Polymer Chemistry*; Cornell University: Ithaca, NY, 1953; Chapters 10 and 12.
- (3) (a) Kruse, W. A.; KIRSTE, R. G.; Haas, J.; Schmitt, B. J.; Stein, D. J. *Makromol. Chem.* **1976**, *177*, 1145. (b) Jelenic, J.; KIRSTE, R. G.; Oberthür, R. C.; Schmitt-Strecker, S.; Schmitt, B. J. *Makromol. Chem.* **1984**, *185*, 129. (c) Dettenmaier, M.; Macconnachie, A.; Higgins, J. S.; Kausch, H. H.; Nguyen, T. Q.; *Macromolecules* **1986**, *19*, 773. (d) Schmitt, B. J.; KIRSTE, R. G.; Jelenic, J. *Makromol. Chem.* **1980**, *181*, 1655. (e) KIRSTE, R. G.; Kruse, W. A.; Ibel, K. *Polymer* **1975**, *16*, 120.
- (4) (a) Ben Cheikh Larbi, F.; Leloup, S.; Halary, J. L.; Monnerie, L. *Polym. Comm.* **1986**, *27*, 23. (b) Bates, F. S.; Wignall, G. D. *Macromolecules* **1986**, *19*, 932.
- (5) (a) Fitzgibbon, P. D.; Frank, C. W. *Macromolecules* **1982**, *15*, 733. (b) Gelles, R.; Frank, C. W. *Macromolecules* **1983**, *16*, 1448. (c) Semerak, S. N.; Frank, C. W. *Can. J. Chem.* **1983**, *63*, 1328.
- (6) (a) Morawetz, H.; Amrani, F. *Macromolecules* **1978**, *11*, 281. (b) Morawetz, H. *Pure Appl. Chem.* **1980**, *52*, 277.
- (7) (a) Ediger, M. D.; Fayer, M. D. *Macromolecules* **1983**, *16*, 1839. (b) Ediger, M. D.; Domingue, R. P.; Peterson, K. A.; Fayer, M. D. *Macromolecules* **1985**, *18*, 1182.
- (8) Peterson, K. A.; Fayer, M. D. *J. Chem. Phys.* **1986**, *85*, 4702.
- (9) (a) Gochanour, C. R.; Andersen, H. C.; Fayer, M. D. *J. Chem. Phys.* **1979**, *70*, 4254. (b) Loring, R. F.; Andersen, H. C.; Fayer, M. D. *J. Chem. Phys.* **1982**, *76*, 2015.
- (10) Galanin, M. D. *Tr. Fiz. Inst. I. P. Pavolova* **1950**, *5*, 341.
- (11) Flory, P. J. *Statistical Mechanics of Chain Molecules*; Interscience: New York, 1969.
- (12) (a) Haan, S. W.; Zwanzig, R. *J. Chem. Phys.* **1978**, *68*, 1879. (b) Klafter, J.; Silbey, R. *J. Chem. Phys.* **1980**, *72*, 843. (c) Godzik, K.; Jörtner, J. *J. Chem. Phys.* **1980**, *72*, 4471.
- (13) (a) Huber, D. L. *Phys. Rev. B: Condens. Matter* **1979**, *20*, 2307. (b) Huber, D. L. *Phys. Rev. B; Condens. Matter* **1979**, *20*, 5333.
- (14) (a) Fredrickson, G. H.; Andersen, H. C.; Frank, C. W. *Macromolecules* **1983**, *16*, 1456. (b) Fredrickson, G. H.; Andersen, H. C.; Frank, C. W. *Macromolecules* **1984**, *17*, 54. (c) Fredrickson, G. H.; Andersen, H. C.; Frank, C. W. *J. Polym. Sci., Polym. Phys. Ed.* **1985**, *23*, 591.
- (15) Ediger, M. D.; Fayer, M. D. *J. Chem. Phys.* **1983**, *78*, 2518.
- (16) Baumann, J.; Fayer, M. D. *J. Chem. Phys.* **1986**, *85*, 4087.
- (17) Förster, Th. *Ann. Phys. (Leipzig)* **1948**, *2*, 55.
- (18) (a) Gochanour, C. R.; Fayer, M. D. *J. Phys. Chem.* **1981**, *85*, 1989. (b) Steinberg, I. Z. *J. Chem. Phys.* **1968**, *48*, 2411. (c) Blumen, A. *Ibid.* **1981**, *74*, 6926.
- (19) Fox, T. G.; Kinsinger, J. B.; Mason, H. F.; Schuele, E. M. *Polymer* **1962**, *3*, 71.
- (20) Hayashi, H.; Flory, P. J.; Wignall, G. D. *Macromolecules* **1983**, *16*, 1328.
- (21) Brandrup, J.; Immergut, E. H., Eds. *Polymer Handbook*; Wiley: New York, 1975; section IV.